

Carbon fiber-based long-gauge sensors monitoring the flexural performance of FRP-reinforced concrete beams

Mohamed A. Saifeldeen* and Nariman Fouad^a

Department of Civil Engineering, Faculty of Engineering, Aswan University, Egypt

(Received November 18, 2023, Revised December 17, 2023, Accepted December 20, 2023)

Abstract. Long-gauge carbon fiber line (CFL) sensors have received considerable attention in the past decade. However, there is still a need for an in-depth investigation of their measuring accuracy. This study investigates the accuracy of carbon fiber line sensors to monitor and differentiate the flexural behavior of two beams, one reinforced with steel bars alone and the other reinforced with steel and basalt fiber-reinforced polymer bars. A distributed set of long-gauge carbon fiber line, Fiber Bragg Grating (FBG), and traditional strain gauge sensors was mounted on the tensile concrete surface of the studied beams to compare the results and assess the accuracies of the proposed sensors. The test beams were loaded monotonically under four-point bending loading until failure. Results indicated the importance of using long-gauge sensors in providing useful, accurate, and reliable information regarding global structural behavior, while point sensors are affected by local damage and strain concentrations. Furthermore, long-gauge carbon fiber line sensors demonstrated good agreement with the corresponding Fiber Bragg Grating sensors with acceptable accuracy, thereby exhibiting potential for application in monitoring the health of large-scale structures.

Keywords: carbon fiber sensors; FBG sensors; flexural behavior; FRP bars; long gauge sensors; strain distribution; structural health monitoring

1. Introduction

The strategy of damage identification process for civil engineering infrastructures is referred to as structural health monitoring (SHM), which mainly includes detection of localized damage and the overall structural response. An observation of a structural behavior using periodically spaced measurements is involved in this process (Ansari 2005, Farrar and Worden 2010). Damage is delineated as alterations introduced into a system that have an adverse impact on the current or prospective performance of that system, potentially compromising its functionality and overall effectiveness. Damages of a reinforced concrete structure can be occurred due to various parameters such as; reinforcement corrosion or excessive loads. As part of maintaining and repairing concrete structures in service, as well as monitoring hazards arising from concrete structures, detection of damage involves monitoring crack presence, location, and evaluation, reinforcement corrosion, material behavior, and local stress/strain concentrations of engineering importance. Over the past two decades, the published researches on SHM has significantly increased. Researchers have been

*Corresponding author, Assistant Professor, E-mail: mohamed.saifeldeen@aswu.edu.eg

^a Assistant Professor, E-mail: nariman.fouad@aswu.edu.eg

motivated to conduct research in the field SHM due to the increasing interest in this area and the potential benefits it can provide in terms of life safety and economic gains (Worden and Dulieu-Barton 2004, Ko and Ni 2005, Glisic and Inaudi 2007).

Numerous methods for SHM have been suggested in recent decades. Among the prevalent approaches are vibration-based monitoring, strain monitoring, and monitoring based on elastic waves, acoustic emission, ultrasonic inspection, Eddy current, and electromechanical impedance-based monitoring. Vibration-based and strain-based techniques are widespread common techniques for SHM (Wang and Yang 2017). The fundamental idea behind vibration-based techniques is that alterations in the mechanical properties of a structure manifest as changes in its dynamic characteristics, allowing for their detection. When applying vibration-based techniques to real structures, observed uncertainties in measurements are often attributed to factors such as noise, fluctuations in temperature, and the specific excitation mechanisms inherent in the structure. (Ercolino *et al.* 2015). Recently, several studies have been undertaken to enhance the reliability of measurements. Most of the vibration-based techniques such as accelerometers used mainly for global monitoring of structures, however the global properties are not significantly affected by low levels of damages. Strain-based sensing techniques are effective to detect local damages and more sensitive to small-scale damage. Using appropriate system of distributed strain sensors, global monitoring of large scale structures can be conducted efficiently.

Measurements of strain using traditional point-strain gauges give only local information about the structural. As a result of these limitations, the strain-modal theory is restricted in its application in civil engineering and development. Strain gauges (SGs) must be installed such that they cover at least the vicinity of the damaged area to prevent failure in damage identification (Zhang *et al.* 2015, Fouad *et al.* 2016). Traditional SGs as point sensors are not applicable to large-scale and complex structures, because covering the entire structure is highly expensive. Therefore, point-strain sensors are not suitable for damage detection of civil structures (Abdel-Jaber and Glisic 2014, Wu *et al.* 2018). Nonetheless, SGs prove advantageous and are more suitable than long gauge sensors when it comes to monitoring the responses of diminutive structures like anchorage structures, owing to their compact size (Abdullah *et al.* 2015, Dang *et al.* 2020). Long-gauge strain sensors possess a distinctive capability to capture both localized and overarching structural information. This is achieved by measuring the average strain across the sensor's covered area (gauge length). The emergence of the long-gauge strain sensor provides a new opportunity for the advancement of the theory related to the identification of macro-strain modal. This sensor can reveal the global information of the structures because its gauge length ranges from the order of a few centimeters to an effective gauge length extending up to several meters (Hong *et al.* 2017, Chen *et al.* 2019; Hong *et al.* 2020).

The utilization of carbon fibers (CFs) has been explored and applied in both industrial and construction settings. Capitalizing on their impressive mechanical characteristics, CFs can be crafted with epoxy resin to produce various structural reinforcements, including sheets and rods of carbon fiber-reinforced polymer (CFRP). (Hollaway 2010, Siddika *et al.* 2019). Owing to their electrical properties, the CFRP composites exhibit the ability of strain sensing (Chung 2012, Huang and Wu 2012). In addition, it has been recognized that CFRP composites can serve as a dual-purpose material for strengthening and self-sensing. This involves the detection of potential damages in CFRP or CFRP-strengthened structures, leveraging the electrical conductivity and piezoresistivity of CFRPs.

Previous studies have demonstrated that CF sensors are fabricated to measure the strain changes in structures, and demonstrate good stability in measuring low and high level strains (Yang *et al.* 2007, Hu *et al.* 2010, Huang *et al.* 2012, Fouad and Saifelddeen 2021).

The continuous carbon fiber (CF) tow is composed of numerous uninterrupted microfibers, each functioning as an individual sensing cell. The output signal of the CF sensor is a cumulative response from all these sensing cells. The change in the resistance ratio ($\Delta R/R$) of a CF sensor is directly proportional to changes in strain. The CF sensor can effectively measure strains with a satisfactory linearity and repeatability till 6000 micro-strains with fluctuation errors varied between ± 3.5 micro-strains (Saifeldeen *et al.* 2016, Saifeldeen *et al.* 2017). In the field of SHM, CF sensors present several benefits. They are well-suited for measuring strain in large-scale structures, possess durability and resistance to rust, and demonstrate high strength, ensuring long-term stability without degradation. Furthermore, carbon fibers (CFs) can function as both strengthening and self-sensing materials. Moreover, the manufacturing of CF sensors is more cost-effective compared to other optical sensor types.

Extensive research has explored the utilization of fiber-reinforced polymer (FRP) materials to retrofit and repair damaged concrete structures due to their exceptional properties. The mechanical and material attributes of FRP composites, including corrosion resistance, high strength, lightweight, durability, and elasticity, render them appealing for strengthening applications. (Zureick *et al.* 2006, Li *et al.* 2017, Pham and Hao 2017, Naser *et al.* 2019). The implementation of FRP bars as an alternative to conventional steel reinforcements in reinforced concrete structures has gained considerable acceptance in the construction field (Kassem *et al.* 2011). FRP bars are manufactured from a non-corrosive material, making them ideal for reinforcing concrete structures in cruel environments. A prominent challenge observed in flexural members reinforced with basalt FRP (BFRP) bars is their tendency to display brittle behavior. Unlike materials that undergo yielding, BFRP bars maintain linear elastic behavior until reaching the point of failure. This could lead to abrupt failure without prior indication, an outcome deemed unacceptable by designers. Given the potential to enhance concrete properties, it is advisable to design FRP-reinforced concrete members to fail through concrete crushing rather than bar rupture. (Abed and Alhafiz 2019, Lu *et al.* 2020; Zou *et al.* 2020).

This study aims to develop high-performance long-gauge carbon fiber line (CFL) sensors for practical adaptation in civil SHM. The proposed CFL sensors have been developed and verified to have the ability to obtain effective macro-strain distributions. In this study, an experimental investigation was conducted to analyze the effectiveness of the proposed CFL sensors in identifying the flexural characteristics of various structure types. The CFL and Fiber Bragg Grating (FBG) long-gauge sensors were compared to determine the reliability of the measuring strains of the CFL sensors. In addition, the importance of using long-gauge sensors in monitoring structures in comparison with traditional point sensor SGs was discussed.

2. Fundamentals of strain measurement

2.1 Carbon fiber sensors

The measurement of strain using a CF sensor relies on establishing a correlation between the ratios of electrical resistance change ($\Delta R/R$) and the applied strains (ϵ). Carbon functions as a semiconductor material with low conductivity. To assess the variation in electrical resistance, a Wheatstone bridge measuring circuit was employed, measuring the change in electrical resistance of the sensor ($\Delta R/R$). The correlation between $\Delta R/R$ and the applied strain is outlined as follows

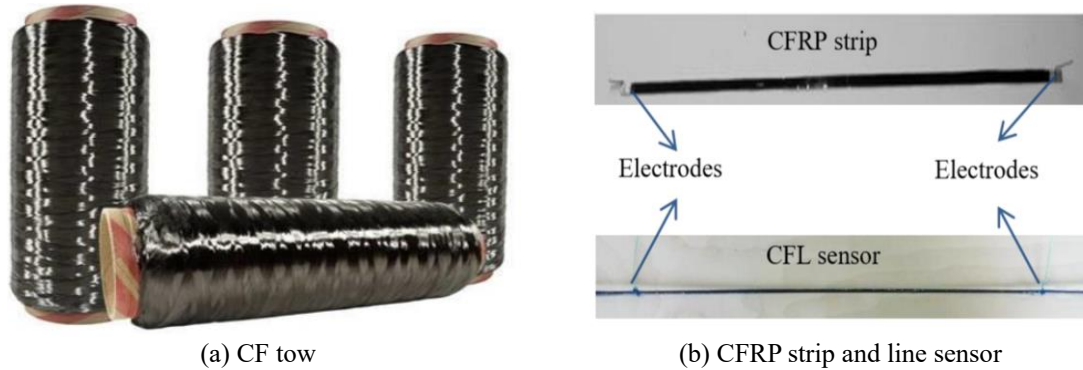


Fig. 1 Photographs of CFRP sensor

$$\varepsilon = \left(\frac{\Delta R}{R} \right) / GF \quad (1)$$

where GF denotes the gauge factor, the measuring mechanism was discussed in detail by (Huang, *et al.* 2012; Saifelddeen *et al.* 2017). A long-gauge CFRP strip sensor for strain measurements has been developed by (Huang *et al.* 2012). The width of the sensor was approximately 6 mm, and the gauge length was 500 mm. The distance between the two fixed electrodes represented the effective sensing part of the sensor. The strip sensor has been upgraded by (Saifelddeen, Fouad *et al.* 2017) to produce a CFL sensor with a diameter of less than 1.4 mm using a carbon fiber tow with a width of 6 mm. The photographs of the CF tow, proposed CFRP strip, and CFL sensor are depicted in Figs. 1(a) and 1(b). By employing a double-tensioning method, (Saifelddeen *et al.* 2016) improved the precision of CFL sensors in low strain measurements. The sensor exhibited a consistent signal, providing accurate strain measurements in relation to the reference strain, with fluctuation errors ranging within $\pm 3.5 \mu\varepsilon$. The adoption of the double-tension approach notably elevated the sensors' performance, particularly with short gauge lengths of up to 100 mm.

2.2 Fiber Bragg grating sensors

Owing to their rapid advancement in recent years, fiber optic sensing technologies have drawn considerable interest and are regarded as notable advancements in the innovation of sensing techniques. The FBG sensor yields high precision in static and dynamic measurements, and is anticipated to emerge as one of the most prospective fiber optic sensors. Over recent years, the FBG sensor has undergone development for diverse measurements, including strain, temperature, acceleration, and crack width. (Glisic *et al.* 2013). Numerous studies (Li and Wu 2007, Tang and Wu 2016, Chen *et al.* 2017) have effectively employed distributed long-gauge FBG sensors to monitor strain distributions across entire or crucial areas of structures and deflections, exhibiting superior performance compared to that of Small-Scale Models (SGs).

3. Experimental setup

3.1 Specimens and materials properties

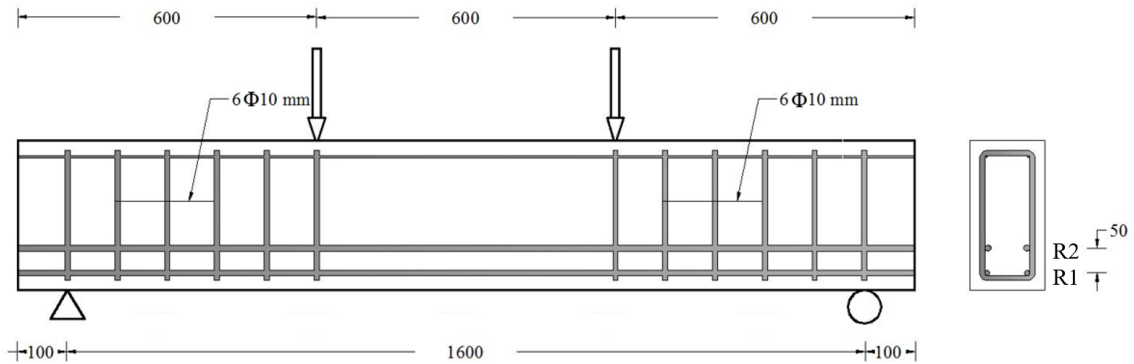


Fig. 2 Cross-section and longitudinal section of test beams with reinforcement details

Table 1 Details of reinforcement

Beam index	Main reinforcements	
	R1	R2
SS-50	2 ϕ 10 mm steel bars	2 ϕ 13 mm steel bars
SB-50	2 ϕ 10 mm BFRP rods	2 ϕ 13 mm steel bars

Table 2 Mechanical properties of steel and FRP materials

Material type	Elastic modulus		Yield stress		Tensile strength	
	E (GPa)		f_y (MPa)		f_u (MPa)	
	average	C.O.V.	average	C.O.V.	average	C.O.V.
Longitudinal steel bars	200	0.75%	375	2.7%	560	3.6%
Stirrup steel bars	200	0.9%	400	3.8%	625	4.2%
10-mm-diameter BFRP bars	48.1	1.9%	-----	-----	1113	3.9%

Two simply supported reinforced concrete beams (SS-50 and SB-50) with a total length of 1800 mm and a clear span of 1600 mm were tested under a four-point loading test. The cross-sections of the beams had a rectangular shape with a width of 150 mm and a depth of 300 mm. The concrete mix was a ready mix concrete provided by a company with a compressive strength of 30 Mpa, according to the datasheet provided by the company. Stirrups were also considered throughout the entire length of the specimen except for the middle section, with a 10 mm diameter and 80 mm pitch. The details of the beams and reinforcement are shown in Fig. 2 and Table 1. The average mechanical characteristics of the steel reinforcement and BFRP materials and the coefficient of variation of three tested specimens (C.O.V.) are listed in Table 2.

3.2 Sensor configurations

To demonstrate the effectiveness of the proposed long-gauge CFL sensors in monitoring the flexural behavior of reinforced concrete beams, five CFL sensors with a 300 mm gauge length were

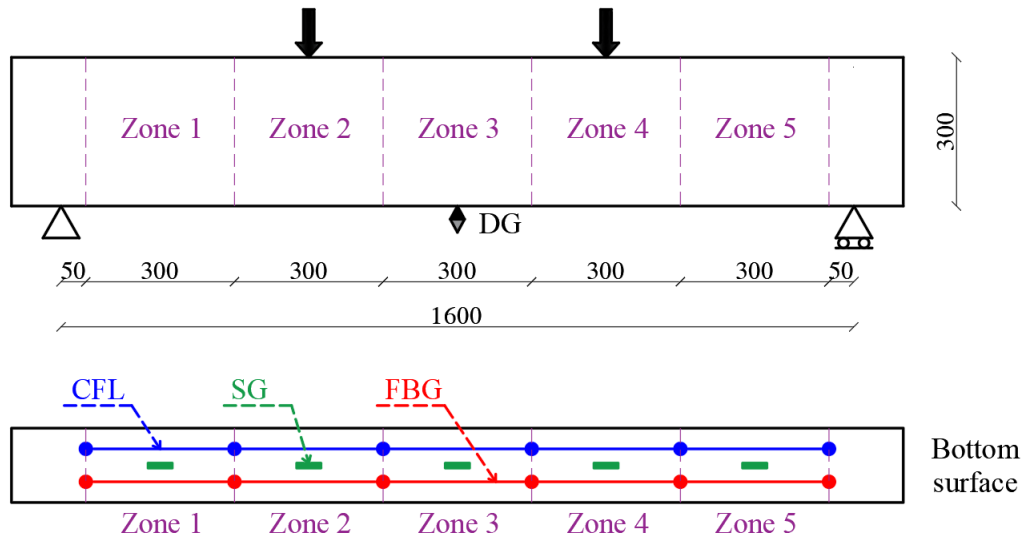


Fig. 3 Sensor placement on bottom concrete surface



(a) During setup



(b) After failure

Fig. 4 Tested beam

arranged in series on the bottom surface of the beam to implement a quasi-distributed measurement, as depicted in Fig. 3. A set of five FBG sensors having same gauge length, 300 mm, were mounted at the same locations as the CFL sensors for comparison. In addition, another set of five traditional SGs with a gauge length of 60 mm were installed in the middle of each sensor to distinguish the performance between the long-gauge (CFL and FBG) and point (SG) sensors. A displacement gauge (DG) was installed at the mid-span of the specimen to provide an index to verify the global behavior of the structure. The concrete surface was prepared by removing the cement cover using a diamond sander, subsequently, an epoxy primer was administered following the cleaning of the concrete surface with acetone. Next, all long-gauge sensors were bonded to the concrete surface from both ends only using epoxy adhesive. For ease of discussion, the region with sensor installation was partitioned into five zones, identified as zones 1–5.



Fig. 5 Schematic of crack propagation at failure: (a) SS-50 and (b) SB-50

3.3 Loading setup

The specimens were subjected to four-point bending loading with a load span of 600 mm. The loading and measuring setup is illustrated in Fig. 4, wherein a hydraulic universal testing machine was used to load the beams. Using a transferred steel board, the load applied by the loading machine was equally divided into two parts. The progressively increasing load was applied monotonically in a load-controlled mode up to failure. To detect the subtle changes before and after the occurrence of the first several cracks, the upload was performed at a significantly low speed (5 kN/min) below 30 kN, where 20 kN was determined to be the cracking load based on theoretical calculation. After that, the loading rate increased to 10 kN/min till failure.

4. Test results and discussions

4.1 Flexural behavior of tested beams

The crack propagation of SS-50 and SB-50 after complete failure is depicted in Fig. 5. From this figure, the following observations can be drawn: (i) The first crack in both tested beams manifested on the underside within the constant moment region near the applied load. Subsequently, multiple flexural tension cracks emerged across the constant moment zone. Although the number of cracks increased, they did not widen during the loading process and maintained smaller widths for SB-50 than those for beam SS-50. (ii) No clear difference was observed in the first crack loads of both beams, which were 22 kN and 24 kN for SB-50 and SS-50, respectively. However, there was an obvious difference in their peak loads, which were 182 kN and 161 kN for SB-50 and SS-50, respectively. (iii) The failure of the beam reinforced with BFRP bars occurred due to the compression zone's concrete crushing.; in contrast, the failure mode of the beam reinforced with steel bars alone was flexural failure.

The correlation between the applied load and mid-span deflection for the examined beams is depicted in Fig. 6. From this figure, it can be seen that the beam SS-50 exhibits a larger stiffness than that of SB-50. Both beams have approximately the same ductility; however, the loading curve of beam SB-50 undergoes a sharp drop after the peak load as a result of collapsing in the compression zone. For SS-50, the steel bars exhibited yielding at deflection and a load of 4.5 mm and 142 kN, respectively. The mid-span deflection increased significantly with a slight increase in the applied load. However, in the case of SB-50, the slope of the load–deflection curve deviated at a deflection and load of 5.5 mm and 125 kN, respectively, which indicates the yielding of steel reinforcement. Subsequently, a continuous increase in the applied load with a greater increase in deflection was observed as a benefit because BFRP bars have no yielding stage.

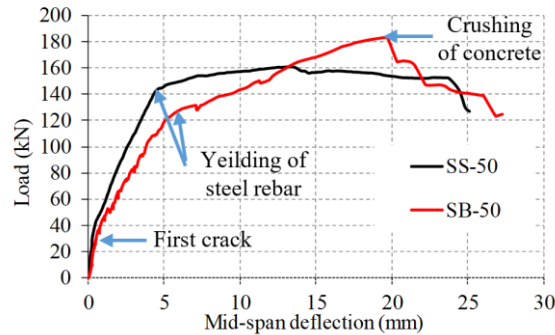


Fig. 6 The correlation between the applied load and mid-span deflection for the examined beams

4.2 CFL sensors for crack detection

Considering the two types of long-gauge strain sensors of a 300 mm gauge length utilized in this study, along with SGs of 60 mm length, the measured results for crack detection for beam SB-50 in each zone for these sensors are depicted in Fig. 7. From this figure, the first crack in each zone can be recognized as follows: (i) The first crack occurred in zone 2 at a load of 22 kN, and the second crack occurred in zone 3 at a load of 23 kN. The measured macro-strains using long-gauge CFL and FBG sensors abruptly increased as a result of crack occurrence, while there were no obvious changes in the strain measured using traditional SGs. This was because the cracks were located outside the sensing range of the SGs (see Fig. 8). (ii) The third crack initiated in zone 4 at a load of 24 kN. The CFL and FBG sensors, as well as the traditional SGs could identify this crack, as it passed through the gauge length of each of them (see Figs. 7 and 8). (iii) At an applied load of 33 kN, additional cracks occurred simultaneously in zones 1 and 5, where the CFL, FBG, and SG sensors identified the crack initiated in zone 5; however, only long-gauge sensors could detect the other cracks in zone 1.

From the measured strains in zones 4 and 5 depicted in Fig. 7, in the case of long-gauge sensors (CFL and FBG), the change in the measured macro-strains is lesser than that for the point gauge (SGs) when the crack manifests. This matches with the concept, the long-gauge sensors measure the average macro-strains within its gauge length, which is less sensitive to the local stress or strain concentration and more representative of the overall behavior of the structural member. Furthermore, the traditional SG as a point sensor can only identify cracks passing through its short gauge length; thus, it is extremely expensive to cover the entire structure with SG sensors. In addition, the measured strain response of SG sensors to damage shows significant changes in comparison with the severity of the crack, which can be considered to be a misleading result.

4.3 CFL sensors for structural performance evaluation

The macro-strain responses recorded by various sensors during monotonic loading until reaching the ultimate load for the examined beams are illustrated in Fig. 9. The strain measurements of the CFL sensors demonstrate good sensitivity to the applied load at low and high strain levels. In addition, the proposed sensors match well with the corresponding strains of the long-gauge FBG sensors with the same gauge length. However, there exist some differences in the measured strains

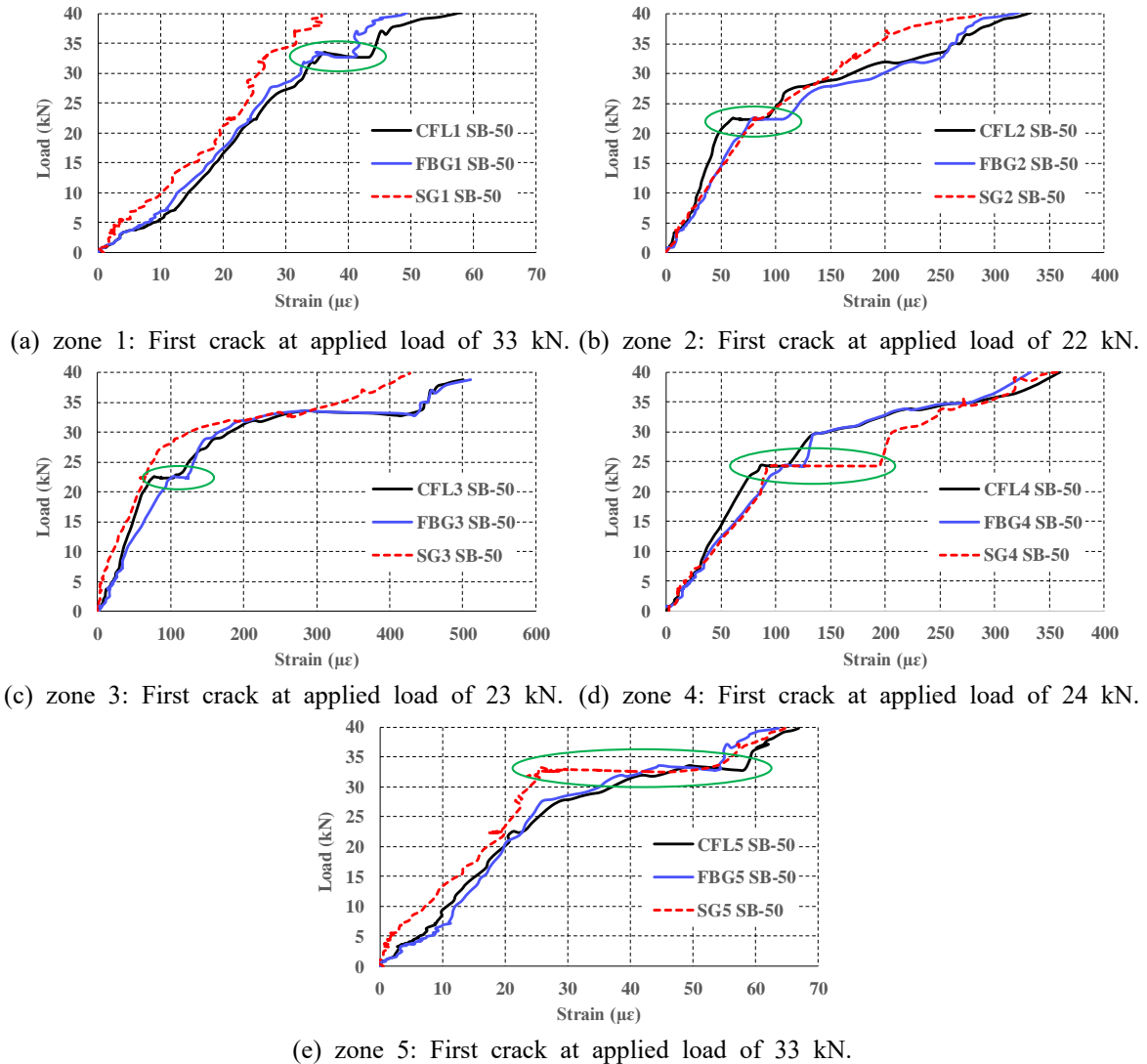


Fig. 7 Crack detection based on strain measurement of different sensors.

between the long-gauge sensors and the SG point sensors, particularly following crack propagation. In addition, there is a clear similarity between the recorded strains of the sensors at locations 1 and 2 with those measured at locations 5 and 4, respectively, particularly before and after the occurrence of slight cracks. This indicates the accuracy of the measured strains of the proposed CFL sensors. By comparing the measured strains and the overall behaviors of the two tested beams, it can be seen that, at the same load level, the measured strains from SB-50 reinforced with BFRP bars have larger values than those recorded from SS-50, as the modulus of elasticity of BFRP bars is less than that of the steel bars, as validated by the load–deflection curve above (Fig. 6). The readings taken from the CFL, FBG, and SG sensors were reasonable up to the ultimate load of each beam. This can be attributed to the instability of the sensor fixation positions after reaching this loading level, which

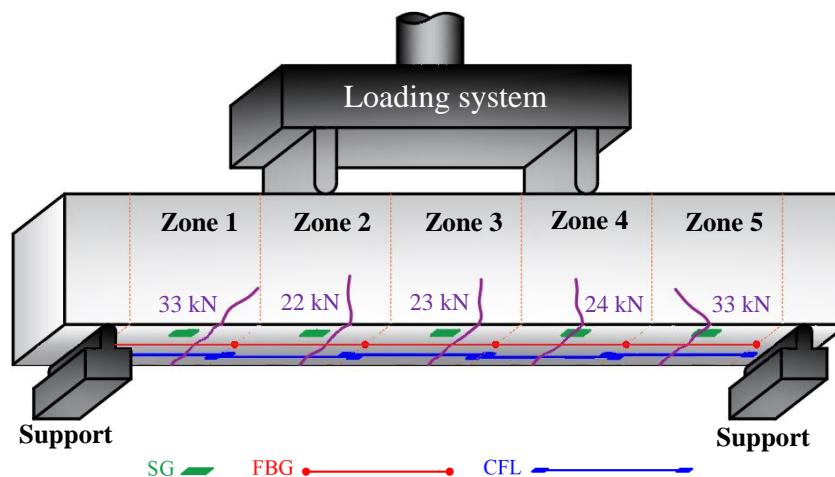


Fig. 8 Schematic indicating the location of first crack in each zone

affects the accuracy of the measured strains.

The recorded strain values from SGs consistently appear smaller than those from long gauge sensors. This difference implies that certain cracks may have occurred beyond the gauge length of the SGs but within the range of the long gauge sensors. In light of this experiment, it becomes clear that all sensors are proficient in determining the three phases of concrete (elastic, plastic, and damage). This is attributed to the relatively short length of the tested beam (1.8 m), which can be considered a small-scale structure relative to the gauge length of SGs. However, in the case of large-scale structures, long gauge sensors exhibit the ability to detect all cracks occurring within their gauge length, a capability not consistently replicated by SGs, leading to occasional unreliability in strain values.

Fig. 10 depicts the strain distributions measured by different sensors along the length of the tested beams. The measured strains for the CFL, FBG, and SG sensors were recorded at 20 kN intervals up to 140 kN and 160 kN for SS-50 and SB-50, respectively, for each zone to obtain the macro-strain distribution along the beams to reveal the efficiency of the different sensors in monitoring the flexural behavior of the reinforced concrete structure. There was a notable concurrence in the strain distributions recorded by both CFL and FBG sensors. From lower to higher load levels. In contrast, the alternative strain distributions obtained using the SG sensors demonstrated some divergence as they were more sensitive to local cracks. For SS-50, the recorded strain distributions increased proportionally with the applied load up to 140 kN (before yielding of the steel rebar). For SB-50, the same trend was observed up to 120 kN, and then an abrupt increase in strain distribution was seen as the steel rebar yielded at 125 kN and the BFRP bars had no yielding stage.

4.4 Comparison between strain distributions of all sensors

For each zone, the three types of sensors (CFL, FBG, and SG) compared with each other at each load level to reveal the efficiency of the different sensors. Fig. 11 depicts the relationship between the strain distributions, which plotted in Fig. 10, measured using different sensors. A linear relationship was found between the CFL and FBG sensors mounted on the concrete surface wherein

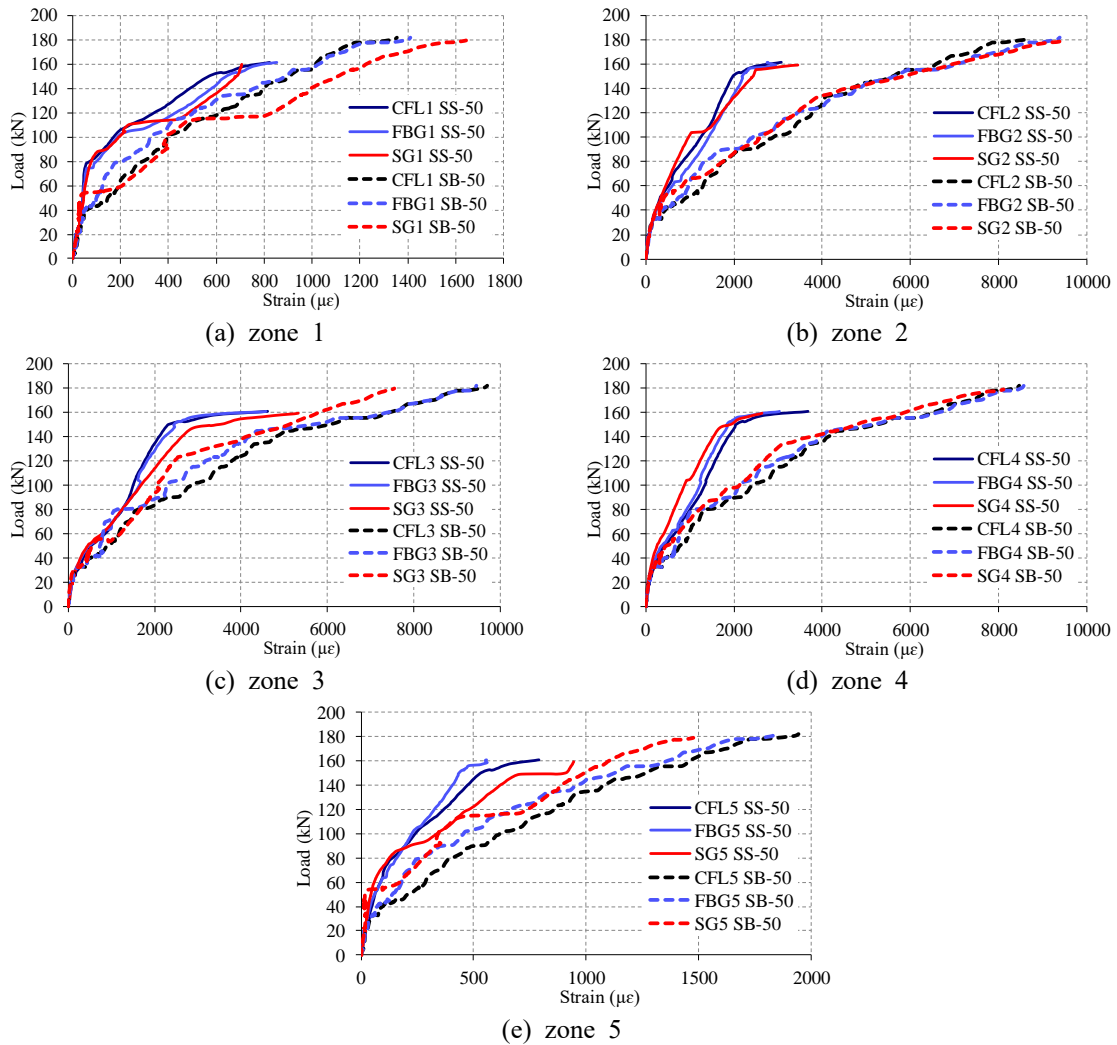


Fig. 9 Macro-strain responses obtained using different sensors under monotonic load for tested beams

the values of the coefficient of determination (R^2) were close to 1 for both the tested beams at the different stages of the applied load until failure. This proves the reliability and accuracy of the proposed CFL sensors in monitoring various types of structures. From the relationship between the strain distributions measured using the different long-gauge sensors and traditional SGs, there were some outlier values that caused loss of linearity, as can be identified from the calculated R^2 values.

5. Conclusions

This study proposed a novel technique for macro-strain measurements based on a long-gauge CFL sensor. CFL sensors provide several advantages in the realm of SHM: they are well-suited for area strain measurements in large-scale structures, exhibit durability and corrosion resistance, and

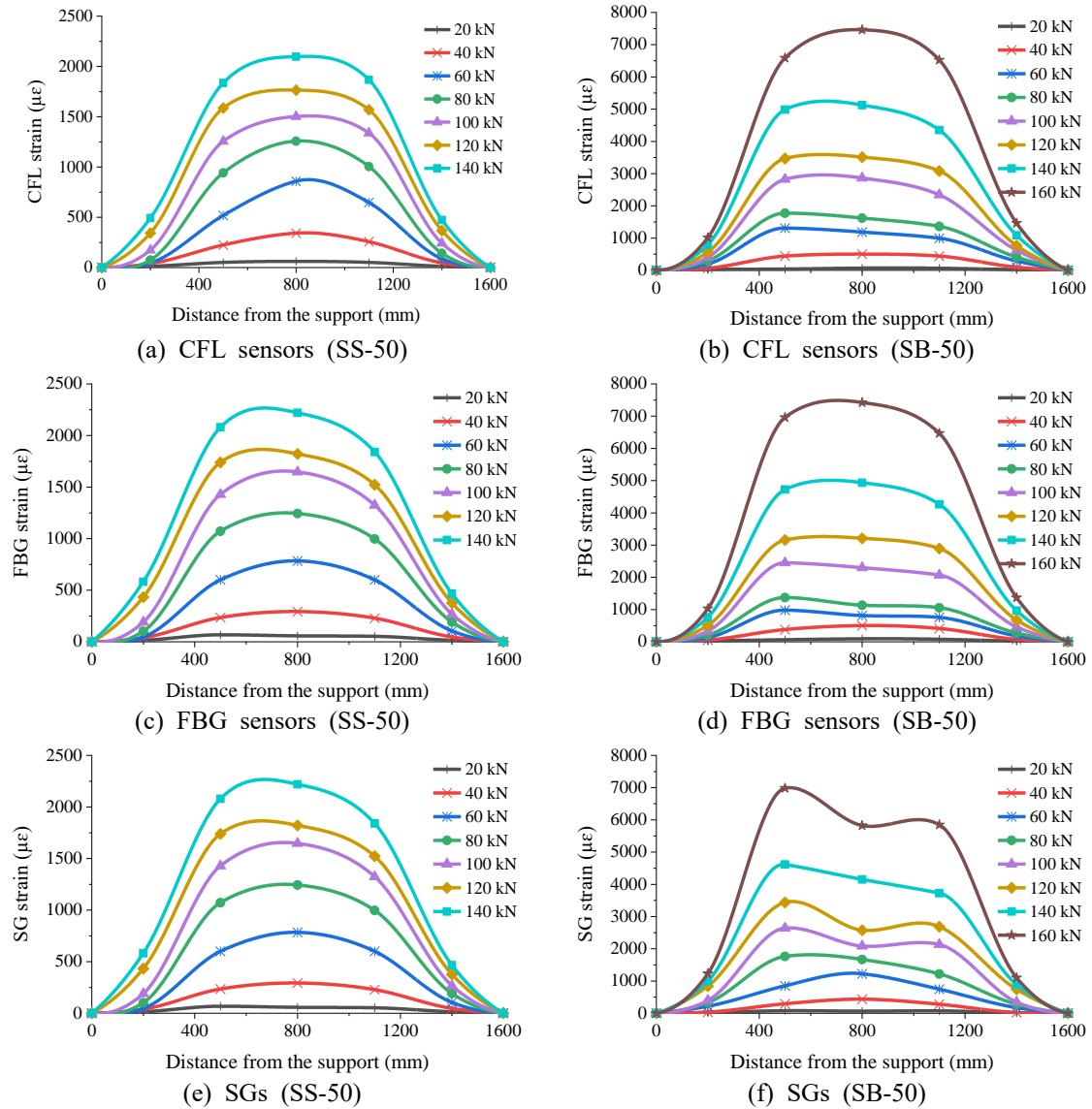


Fig. 10 Strain distributions measured by different sensors along length of tested beams

possess high strength, ensuring long-term stability without degradation. An experimental investigation was performed to study the capability of the proposed CFL sensors to differentiate the flexural behavior of two beams, one reinforced with steel bars alone, and the other beam reinforced with steel and BFRP bars. Based on the experimental results, the following important conclusions can be drawn:

- At the same load level, the measured strains and mid-span deflection for SB-50 strengthened with BFRP bars exhibited larger values than those recorded for SS-50, as the modulus of elasticity of BFRP bars was less than that of steel bars.

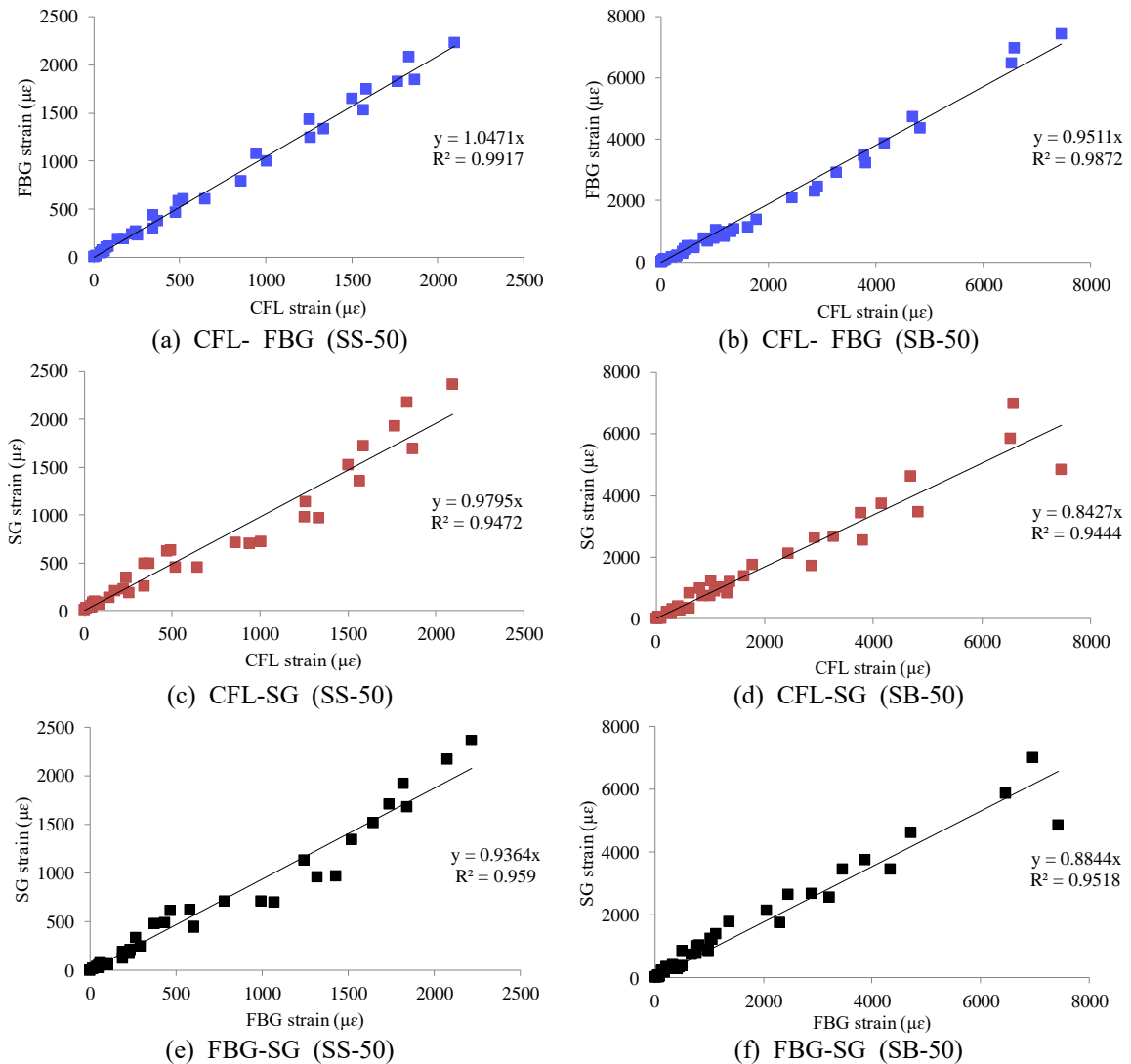


Fig. 11 Relationship between strain distributions measured using different sensors

- Long-gauge CFL sensors exhibited good agreement with the corresponding FBG sensors with acceptable accuracy, demonstrating potential for application in monitoring the health of large-scale structures.
- The distributed long-gauge CFL and FBG sensors could detect the occurrence of first cracks within its gauge length effectively.
- The proposed long-gauge sensors could measure the average macro-strains within their gauge length, acquire measurements without accounting for the impact of localized cracks, and determine the global behavior of the structures.
- The traditional SG as a point sensor could only identify cracks passing through its small gauge length; consequently, it is significantly expensive to cover the entire structure with SG point sensors. Furthermore,

the measured strain response to damage resulted in significant changes compared to the severity of the cracks.

Both FBG and CFL long gauge sensors are accurate, durable, rustproof, and offer stability for long-term service without deterioration. Still, CF sensors provide extra advantages; they have the potential for utilization as both a strengthening and self-sensing material, less likely to be damaged as it high strength material and more economical than optical sensors.

Future work

Measured strain responses can be used to quantify applied values in reinforced concrete structures, strain measurements provide valuable information about the deformation and stress experienced by the material. In reinforced concrete structures, strain gauges or sensors are often strategically placed to monitor the strain in critical locations. By analyzing the measured strain responses, engineers can infer the applied loads, stresses, and deformation patterns within the structure. This information is crucial for assessing the structural health, performance, and safety of reinforced concrete elements. The data obtained from strain measurements can be used to validate design assumptions, identify potential structural issues, and optimize the design for efficiency and safety.

In summary, measured strain responses serve as a valuable tool for quantifying applied loads and assessing the behaviour of reinforced concrete structures, contributing to the overall understanding and management of structural integrity.

Funding

This research received no specific grant from any funding agency in the public, commercial, or not-for-profit sectors.

Declaration of conflicting interests

The Author(s) declare(s) that there is no conflict of interest.

References

- Abdel-Jaber, H. and Glisic, B. (2014), "A method for the on-site determination of prestressing forces using long-gauge fiber optic strain sensors", *Smart Mater. Struct.*, **23**(7), 075004. <https://doi.org/10.1088/0964-1726/23/7/075004>.
- Abdullah, A., Rice, J.A. and Hamilton, H. (2015), "A strain-based wire breakage identification algorithm for unbonded PT tendons", *Smart Struct. Syst.*, **16**(3), 415-433. <https://doi.org/10.12989/sss.2015.16.3.415>.
- Abed, F. and Alhafiz, A.R. (2019), "Effect of basalt fibers on the flexural behavior of concrete beams reinforced with BFRP bars", *Compos. Struct.*, **215**, 23-34. <https://doi.org/10.1016/j.compstruct.2019.02.050>.
- Ansari, F. (2005), "Fiber optic health monitoring of civil structures using long gage and acoustic sensors", *Smart Mater. Struct.*, **14**(3), S1. <https://doi.org/10.1088/0964-1726/14/3/001>.

- Chen, S.Z., Wu, G. and Feng, D.-C. (2019), "Damage detection of highway bridges based on long-gauge strain response under stochastic traffic flow", *Mech. Syst. Signal. Pr.*, **127** 551-572. <https://doi.org/10.1016/j.ymsp.2019.03.022>.
- Chen, S.Z., Wu, G., Xing, T. and Feng, D.C. (2017), "Prestressing force monitoring method for a box girder through distributed long-gauge FBG sensors", *Smart Mater. Struct.*, **27**(1), 015015. <https://doi.org/10.1088/1361-665x/aa9bbe>.
- Chung, D.D.L. (2012), "Carbon materials for structural self-sensing, electromagnetic shielding and thermal interfacing", *Carbon*, **50**(9), 3342-3353. <https://doi.org/10.1016/j.carbon.2012.01.031>.
- Dang, N.L., Huynh, T.C., Pham, Q.Q., Lee, S.Y. and Kim, J.T. (2020), "Damage-sensitive impedance sensor placement on multi-strand anchorage based on local stress variation analysis", *Struct. Control Health Monit.* **27**(7), e2547. <https://doi.org/10.12989/sss.2015.16.3.415>.
- Ercolino, M., Farhidzadeh, A., Salamone, S., Magliulo, G.J.S.M. and Maintenance (2015), "Detection of onset of failure in prestressed strands by cluster analysis of acoustic emissions", *Struct. Monit. Maint.*, **2**(4), 339-355. <https://doi.org/10.12989/smm.2015.2.4.339>.
- Farrar, C.R. and Worden, K. (2010), *An introduction to structural health monitoring*, New Trends in Vibration Based Structural Health Monitoring, Springer.
- Fouad, N. and Saifeldien, M.A. (2021), "Smart self-sensing fiber-reinforced polymer sheet with woven carbon fiber line sensor for structural health monitoring", *Adv. Struct. Eng.*, **24**(1), 17-24. <https://doi.org/10.1177/1369433220944507>.
- Fouad, N., Saifeldien, M.A., Huang, H. and Wu, Z. (2016), "Early corrosion monitoring of reinforcing steel bars by using long-gauge carbon fiber sensors", *J. Civ. Struct. Health Monit.*, **6**(4), 691-701. <https://doi.org/10.1007/s13349-016-0190-7>.
- Glisic, B., Hubbell, D.L., Sigurdardottir, D.H. and Yao, Y. (2013), "Damage detection and characterization using long-gauge and distributed fiber optic sensors", *Opt. Eng.*, **52**(8), 087101. <https://doi.org/10.1117/1.oe.52.8.087101>.
- Glisic, B. and Inaudi, D. (2007), *Fibre optic methods for structural health monitoring*, John Wiley & Sons
- Hollaway, L. (2010), "A review of the present and future utilisation of FRP composites in the civil infrastructure with reference to their important in-service properties", *Constr. Build. Mater.*, **24**(12), 2419-2445. <https://doi.org/10.1016/j.conbuildmat.2010.04.062>.
- Hong, W., Lv, K., Li, B., Jiang, Y., Hu, X., Qu, Q.J.S.M. and Structures (2017), "Deflection determination of concrete structures considering nonlinearity based on long-gauge strain sensors", *Smart Mater. Struct.*, **26**(10), 105023. <https://doi.org/10.1088/1361-665x/aa87d7>.
- Hong, W., Lv, Z., Zhang, X. and Hu, X. (2020), "Displacement shape measurement of continuous beam bridges based on long-gauge fiber optic sensing", *Opt. Fiber Technol.*, **56**, 102178. <https://doi.org/10.1016/j.yofte.2020.102178>.
- Hu, N., Karube, Y., Arai, M., Watanabe, T., Yan, C., Li, Y., Liu, Y. and Fukunaga, H. (2010), "Investigation on sensitivity of a polymer/carbon nanotube composite strain sensor", *Carbon*, **48**(3), 680-687. <https://doi.org/10.1016/j.carbon.2009.10.012>.
- Huang, H. and Wu, Z. (2012), "Static and dynamic measurement of low-level strains with carbon fibers", *Sens. Actuat. A*, **183**, 140-147. <https://doi.org/10.1016/j.sna.2012.06.006>.
- Huang, H., Yang, C. and Wu, Z. (2012), "Electrical sensing properties of carbon fiber reinforced plastic strips for detecting low-level strains", *Smart Mater. Struct.*, **21**(3), 035013. <https://doi.org/10.1088/0964-1726/21/3/035013>.
- Kassem, C., Farghaly, A.S. and Benmokrane, B. (2011), "Evaluation of flexural behavior and serviceability performance of concrete beams reinforced with FRP bars", *J. Compos. Constr.*, **15**(5), 682-695. [https://doi.org/10.1061/\(asce\)cc.1943-5614.0000216](https://doi.org/10.1061/(asce)cc.1943-5614.0000216).
- Ko, J. and Ni, Y.Q. (2005), "Technology developments in structural health monitoring of large-scale bridges", *Eng. Struct.*, **27**(12), 1715-1725. <https://doi.org/10.1016/j.engstruct.2005.02.021>.
- Li, C., Gao, D., Wang, Y. and Tang, J. (2017), "Effect of high temperature on the bond performance between basalt fibre reinforced polymer (BFRP) bars and concrete", *Constr. Build. Mater.*, **141**, 44-51. <https://doi.org/10.1016/j.conbuildmat.2017.02.125>.

- Li, S. and Wu, Z. (2007), "Development of distributed long-gage fiber optic sensing system for structural health monitoring", *Struct. Health Monit.*, **6**(2), 133-143. <https://doi.org/10.1177/1475921706072078>.
- Lu, Z., Su, L., Xian, G., Lu, B. and Xie, J. (2020), "Durability study of concrete-covered basalt fiber-reinforced polymer (BFRP) bars in marine environment", *Compos. Struct.*, **234**, 111650. <https://doi.org/10.1016/j.compstruct.2019.111650>.
- Naser, M., Hawileh, R. and Abdalla, J. (2019), "Fiber-reinforced polymer composites in strengthening reinforced concrete structures: A critical review", *Eng. Struct.*, **198**, 109542. <https://doi.org/10.1016/j.engstruct.2019.109542>.
- Pham, T.M. and Hao, H. (2017), "Behavior of fiber-reinforced polymer-strengthened reinforced concrete beams under static and impact loads", *Int. J. Prot. Struct.*, **8**(1), 3-24. <https://doi.org/10.1177/2041419616658730>.
- Saifeldeen, M.A., Fouad, N., Huang, H. and Wu, Z. (2017), "Advancement of long-gauge carbon fiber line sensors for strain measurements in structures", *J. Intel. Mat. Syst. Str.*, **28**(7), 878-887. <https://doi.org/10.1177/1045389x16665974>.
- Saifeldeen, M.A., Fouad, N., Huang, H. and Wu, Z.S. (2016), "Stabilization of electrical sensing properties of carbon fiber sensors using pre-tensioning approach", *Smart Mater. Struct.*, **26**(1), 015012. <https://doi.org/10.1088/1361-665x/26/1/015012>.
- Siddika, A., Al Mamun, M.A., Alyousef, R. and Amran, Y.M. (2019), "Strengthening of reinforced concrete beams by using fiber-reinforced polymer composites: A review", *J. Build. Eng.*, **25**, 100798. <https://doi.org/10.1016/j.jobe.2019.100798>.
- Tang, Y. and Wu, Z. (2016), "Distributed long-gauge optical fiber sensors based self-sensing FRP bar for concrete structure", *Sensors*, **16**(3), 286. <https://doi.org/10.3390/s16030286>.
- Wang, J. and Yang, Q.-S. (2017), "Sensor selection approach for damage identification based on response sensitivity", *Struct. Monit. Maint.*, **4**(1), 53-68. <https://doi.org/10.12989/smm.2017.4.1.053>.
- Worden, K. and Dulieu-Barton, J.M. (2004), "An overview of intelligent fault detection in systems and structures", *Struct. Health Monit.*, **3**(1), 85-98. <https://doi.org/10.1177/1475921704041866>.
- Wu, B., Wu, G., Yang, C. and He, Y. (2018), "Damage identification method for continuous girder bridges based on spatially-distributed long-gauge strain sensing under moving loads", *Mech. Syst. Signal. Pr.*, **104**, 415-435. <https://doi.org/10.1016/j.ymsp.2017.10.040>.
- Yang, C.Q., Wu, Z.S. and Huang, H. (2007), "Electrical properties of different types of carbon fiber reinforced plastics (CFRPs) and hybrid CFRPs", *Carbon*, **45**(15), 3027-3035. <https://doi.org/10.1016/j.carbon.2007.09.001>.
- Zhang, J., Guo, S., Wu, Z. and Zhang, Q. (2015), "Structural identification and damage detection through long-gauge strain measurements", *Eng. Struct.*, **99**, 173-183. <https://doi.org/10.1016/j.engstruct.2015.04.024>.
- Zou, X., Lin, H., Feng, P., Bao, Y. and Wang, J. (2020), "A review on FRP-concrete hybrid sections for bridge applications", *Compos. Struct.*, 113336. <https://doi.org/10.1016/j.compstruct.2020.113336>.
- Zureick, A.-H., Bennett, R.M. and Ellingwood, B.R. (2006), "Statistical characterization of fiber-reinforced polymer composite material properties for structural design", *J. Struct. Eng.*, **132**(8), 1320-1327. [https://doi.org/10.1061/\(asce\)0733-9445\(2006\)132:8\(1320\)](https://doi.org/10.1061/(asce)0733-9445(2006)132:8(1320)).